JOURNAL OF VIROLOGY, Nov. 2000, p. 10699–10706 Vol. 74, No. 22
0022-538X/00/$04.00+0


# Viral Vascular Endothelial Growth Factor Plays a Critical Role in Orf Virus Infection

LOREEN J. SAVORY,[1] STEVEN A. STACKER,[2] STEPHEN B. FLEMING,[1] BRIAN E. NIVEN,[3] AND ANDREW A. MERCER[1]*

*Departments of Microbiology[1] and Mathematics and Statistics,[3] University of Otago, Dunedin, New Zealand, and Ludwig Institute for Cancer Research, Royal Melbourne Hospital, Victoria 3050, Australia[2]*

Received 12 June 2000/Accepted 11 August 2000

**Infection by the parapoxvirus orf virus causes proliferative skin lesions in which extensive capillary proliferation and dilation are prominent histological features. This infective phenotype may be linked to a unique virus-encoded factor, a distinctive new member of the vascular endothelial growth factor (VEGF) family of molecules. We constructed a recombinant orf virus in which the VEGF-like gene was disrupted and show that inactivation of this gene resulted in the loss of three VEGF activities expressed by the parent virus: mitogenesis of vascular endothelial cells, induction of vascular permeability, and activation of VEGF receptor 2. We used the recombinant orf virus to assess the contribution of the viral VEGF to the vascular response seen during orf virus infection of skin. Our results demonstrate that the viral VEGF, while recognizing a unique profile of the known VEGF receptors (receptor 2 and neuropilin 1), is able to stimulate a striking proliferation of blood vessels in the dermis underlying the site of infection. Furthermore, the data demonstrate that the viral VEGF participates in promoting a distinctive pattern of epidermal proliferation. Loss of a functional viral VEGF resulted in lesions with markedly reduced clinical indications of infection. However, viral replication in the early stages of infection was not impaired, and only at later times did it appear that replication of the recombinant virus might be reduced.**

Vascular endothelial growth factor (VEGF) is a specific mitogen for vascular endothelial cells and a potent inducer of vascular permeability, and it plays a critical role in the formation of new blood vessels during both vasculogenesis and angiogenesis (reviewed in reference 13). The latter includes angiogenesis associated with tumor formation and a number of other pathological conditions (reviewed in reference 1). Several proteins related in sequence and structure to VEGF (also called VPF, for vascular permeability factor) have been reported. The VEGF family now includes placental growth factor (PlGF), VEGF-B, VEGF-C, and VEGF-D, each of which shows between 30 and 45% amino acid sequence identity with VEGF. The family members are all structurally similar and share a central VEGF homology domain, which contains eight cysteine residues that form part of a cysteine knot motif. The VEGF family members are ligands for a set of mammalian tyrosine kinase receptors (37). VEGF binds and activates both VEGF receptor 1 (VEGFR-1) (Flt-1) and VEGFR-2 (Flk-1 or KDR), while PlGF and VEGF-B bind only VEGFR-1. VEGF-C and VEGF-D bind VEGFR-2 and VEGFR-3 (Flt-4). VEGF and PlGF-2 also appear to interact with a recently discovered neuronal cell guidance receptor, neuropilin 1. Although the functional significance of each of these ligand-receptor interactions remains to be precisely defined, gene targeting studies have demonstrated the requirement of VEGFR-1 and VEGFR-2 for embryonic development. In general terms, it appears that VEGFR-1 plays a role in vascular endothelial differentiation and migration, VEGFR-2 is involved in vascular endothelial mitogenesis, and VEGFR-3 is involved in the regulation of angiogenesis of the lymphatic vasculature.

* Corresponding author. Mailing address: Department of Microbiology, University of Otago, P.O. Box 56, Dunedin, New Zealand. Phone: (64) (3) 4797730. Fax: (64) (3) 4797744. E-mail: andy.mercer@stonebow.otago.ac.nz.

We reported previously that the NZ2 strain of the parapoxvirus orf virus encodes an apparent homolog of VEGF (VEGF-ORFV$_{NZ2}$) (26) and recently showed, along with others, that the viral factor shares some of the functional features of mammalian VEGF (31, 43). These include the ability of purified VEGF-ORFV$_{NZ2}$ to stimulate the proliferation of vascular endothelial cells, to promote vascular permeability, and to bind VEGFR-2 and neuropilin 1. However, the viral VEGF does not recognize VEGFR-1 or VEGFR-3 and, as such, forms a new member of the VEGF family of molecules with a unique profile of receptor recognition. The in vivo activities of this new growth factor have not yet been examined.

*Orf virus* is the type species of the genus *Parapoxvirus* and shares numerous features with other members of the poxvirus family (19, 32). However, the distinctive morphology of parapoxvirus virions and the high G+C content of their genomes (44) suggest that a significant genetic divergence from other genera of this family has occurred. This suggestion has been confirmed by sequence analyses of the 140-kb orf virus genome (14, 30). Orf virus produces pustular dermatitis in humans, sheep, and goats (reviewed in reference 19). Infection is initiated in damaged skin, and lesions progress through stages of erythema, papule, vesicle, pustule, and scab, with infection confined to the epidermis. The pathological features of human and ovine orf virus lesions are the same, and in both hosts infection is confined to the epidermis, with no evidence of systemic spread. The lesions are remarkable for extensive vascular proliferation and dilation as well as marked proliferation of the epidermis, with finger-like projections of the epidermis deep into the dermis (18). The expression of an orf virus-encoded member of the VEGF family of molecules may provide an explanation for some of these observations. No other virus has been reported to encode a VEGF.

In this study, we constructed a recombinant orf virus in which the VEGF-like gene was disrupted and used this construct to examine the activities of VEGF-ORFV$_{NZ2}$ during orf

virus infection of its natural host. In vivo expression of the viral VEGF promoted a strong angiogenic response including erythema, capillary proliferation, and dilation. In addition, these experiments demonstrated an unexpected role for the viral VEGF in epidermal proliferation.

## MATERIALS AND METHODS

**Cells and virus.** Orf virus strain NZ2 (33) and vaccinia virus strain Lister (34) were propagated in primary bovine testis (BT) or ovine testis (LT) cells using Eagle's minimal essential medium containing 10% fetal bovine serum and 5% lactalbumen hydrolysate.

**Construction of recombinant orf virus.** The gene encoding VEGF-ORFV$_{NZ2}$ is located within a 1.45-kb *Sph*I-*Sma*I subfragment of the *Kpn*I E fragment of orf virus (26). The 1.45-kb subfragment was isolated and cloned into pSP70 to generate pVU486. Digestion of pVU486 with *Avr*II and *Bsm*I removed a 123-nucleotide sequence from the VEGF-ORFV$_{NZ2}$ gene and was followed by incorporation of a linker (CTAGGATCCTTTTTATGAATTCCG) which introduced *Bam*HI and *Eco*RI restriction sites and a poxvirus early transcription termination signal. The orf virus sequences flanking the linker were a left arm of 981 bp, consisting of 869 bp upstream of the VEGF coding region followed by the first 112 bp of the VEGF gene, and a right arm of 345 bp, consisting of the terminal 167 bp of the VEGF gene and 178 bp downstream of it. This plasmid was designated pVU487. pVU488 contained the *Escherichia coli* guanosine phosphoribosyltransferase (*gpt*) gene under the control of the orf virus early promoter, PE1 (15), and the *E. coli lacZ* gene under the control of the orf virus late promoter, PF1 (14). The promoter-reporter elements were kindly provided by D. Lyttle and will be described in detail elsewhere. An 812-bp PE1-*gpt* fragment was derived from pVU488 by PCR and ligated into the *Bam*HI site of pVU487. The PF1-*lacZ* element was removed from pVU488 using *Eco*RI and ligated into the *Eco*RI site of pVU487. The final plasmid construct was called pVEGF-Δ.

Recombinant orf virus was generated using a procedure adapted from standard protocols used in the generation of vaccinia virus recombinants (27). BT cells were infected with orf virus at a multiplicity of infection of 0.05 PFU per cell and transfected (Lipofectin; Bethesda Research Laboratories) with pVEGF-Δ 3 h later, and lysates were recovered 5 days postinfection (p.i.). BT cells were infected with dilutions of the lysates calculated to give rise to between 1,250 and 5,000 plaques per 35-mm-diameter culture dish. Putative recombinant plaques were identified 5 days p.i. by their blue phenotype in the presence of 5-bromo-4-chloro-3-indolyl-β-D-galactopyranoside (X-Gal). Putative recombinant clones arose at a frequency of $10^{-4}$. Candidate clones were enriched by successive rounds of plaque purification. An apparently pure recombinant clone obtained after three cycles of plaquing was subjected to three further cycles before a stock was prepared. This clone was called ovVEGF-Δ.

**Molecular characterization of recombinant orf virus.** Viral cores were recovered from lysates of infected BT cells by centrifugation through a sucrose-dextran cushion, and DNA was purified by standard methods (12, 29). Restriction enzyme analyses, Southern blot hybridizations, PCRs, and DNA sequence determinations were performed according to standard methods (16, 29). The primers used in PCRs were as follows: gf1, AGCGCCCGGGATCCATGAAG TTGCTCGTCG; gf2, ACTCGAGGTACCTAGCGGCGTCTTCTGGG; gpt, CCTGTTCAAACCCCGCTTTA; lac, GACAAACTCGGGCAGCGTT; and out, TCACCGAGGCGGAGCCGTT.

**Experimental infection of sheep with orf virus.** Orf virus-naive merino-cross lambs were inoculated on the wool-free region of the inner surface of the hind legs. An approximately 2-cm-long scratch was made in the skin using a bifurcated needle, and $10^6$ PFU of virus in 20 μl of phosphate-buffered saline (PBS) was applied to the scratch. Cell-free suspensions were prepared from 3-mm punch biopsies of infected skin (22), and the viral titer was determined by a plaque assay on BT cells.

**Immunohistochemical staining and quantitation of vascular endothelial cells.** Punch biopsies (5 mm) were fixed in 10% neutral buffered formalin and processed onto paraffin wax. Two 4-μm serial sections were taken from three points, 100 μm apart, in the fixed block. The first of the serial sections was stained with hematoxylin and eosin, and the second was used for immunohistochemical analysis of vascularization. Vascular endothelial cells were identified with a polyclonal rabbit anti-human von Willebrand factor antiserum (Dako). The extent of vascularization was quantified from each of three semiserial sections per lesion by counting the stained cells which fell on any of the 400 intersecting points within a grid (0.5 by 0.5 mm), each side of which was divided by 20 equidistant lines. The areal fraction of dermis vascularized was expressed as the fraction of the intersecting points on which a stained cell fell (42).

**Preparation of viral conditioned medium (CM).** BT cells were infected at a multiplicity of infection of 0.1 PFU per cell and incubated until all cells were clearly infected. LT cells were infected at a multiplicity of infection of 3 PFU per cell and incubated for 24 h. Cells were sedimented at low speed, and the supernatants were filtered twice (0.1-μm-pore-size filters) to remove infectious orf virus.

**VEGF bioassays.** Mitogenic assays were conducted with viral CM and human microvascular endothelial cells (HMVEC) (43). HMVEC were seeded at $10^4$ cells per well and allowed to adhere. Samples of CM diluted to 10% in medium with reduced serum and without growth supplements were added. Proliferation was measured by direct counting of cells 72 h later. The Ba/F3-derived cell line Ba/F3-VEGFR-2-EpoR, expressing a chimeric receptor consisting of the extracellular domain of mouse VEGFR-2 and the transmembrane and cytoplasmic domains of the mouse erythropoietin receptor, was used to determine if CM was capable of binding and activating VEGFR-2 (37). Cells were washed free of interleukin 3 and then resuspended in dilutions of CM from virus-infected cells or from COS-7 cells transiently expressing the mouse VEGF isoform consisting of 164 amino acids, VEGF$_{164}$ (37). Cells were incubated for 48 h, and DNA synthesis was quantified by measuring [$^3$H]thymidine incorporation with a beta counter. The induction of vascular permeability by CM was determined by measuring the extravasation of Evans blue dye in guinea pig skin (Miles assay) (43). Anesthetized guinea pigs were injected intracardially with 500 μl of 0.5% Evans blue dye. CM was diluted 1/5 in PBS (pH 7.2), and 100 μl was injected intradermally to shaved areas on the back of the animal. Five nanograms of purified mouse VEGF$_{164}$ was used as a positive control. The animals were sacrificed after 20 min, the skin was excised, dye was eluted in formamide, and the absorbance at 620 nm was recorded.

## RESULTS

**Disruption of the orf virus VEGF gene.** A recombinant orf virus in which the VEGF-ORFV$_{NZ2}$ gene had been inactivated was constructed by removing 116 bp of the gene, including a region encoding five cysteines critical for maintaining the tertiary structure of VEGF, and replacing this segment with a reporter cassette (see Materials and Methods). A schematic representation of the VEGF region of this recombinant virus, ovVEGF-Δ, is shown in Fig. 1, along with DNA analyses which confirmed its identity.

The recombinant virus was predicted to contain three new *Bam*HI sites resulting in the appearance of three additional fragments of 5,414, 812, and 111 bp. In accordance with this prediction, digestion of ovVEGF-Δ DNA with *Bam*HI revealed a new fragment of 5.4 kb which hybridized with a *lacZ*-specific probe (Fig. 1B). The bands corresponding to the 0.8- and 0.1-kb *Bam*HI fragments were too faint to be seen on the gel, and the predicted 2.2-kb reduction in the size of the 54.3-kb *Bam*HI A fragment (26, 29) was not adequately resolved under standard electrophoresis conditions. The additional DNA incorporated in ovVEGF-Δ did not contain a *Hin*dIII site and was predicted to result in a net increase of 4.2 kb in the size of the *Hin*dIII B fragment (26, 29). Figure 1C reveals the predicted increase in the size of *Hin*dIII-B and also shows that the new fragment hybridized with a probe containing the VEGF gene.

PCR analysis with a variety of primer pairs confirmed the purity of ovVEGF-Δ. A PCR product indicative of an intact VEGF gene (427 bp, primers gf1 and gf2) was produced only when wild-type orf virus (WT) DNA was included in the reaction (Fig. 1D, lane 2). PCRs in which one of the pair of primers was derived from *gpt* or *lacZ* gave rise to the predicted products only when ovVEGF-Δ DNA was used as a template (Fig. 1D, lanes 4 to 9). The identity of each PCR product was confirmed by direct DNA sequencing. These analyses confirmed the integrity of the inserted genetic elements and revealed no evidence of any substantial alteration to other regions of the genome of ovVEGF-Δ.

No differences in plaque morphology were observed between WT and ovVEGF-Δ when they were grown in BT cells. Nor were differences apparent in the kinetics of the appearance of infectious virus in one-step or multicycle growth curves (data not shown).

**VEGF-like activity is not produced by ovVEGF-Δ.** CM prepared from cells infected with WT, ovVEGF-Δ, or the Lister strain of vaccinia virus or mock infected with PBS was subjected to three assays of VEGF-like activity: endothelial cell mitogenesis, vascular permeability, and activation of VEGFR-2. CM from WT-infected LT cells was able to promote a three-

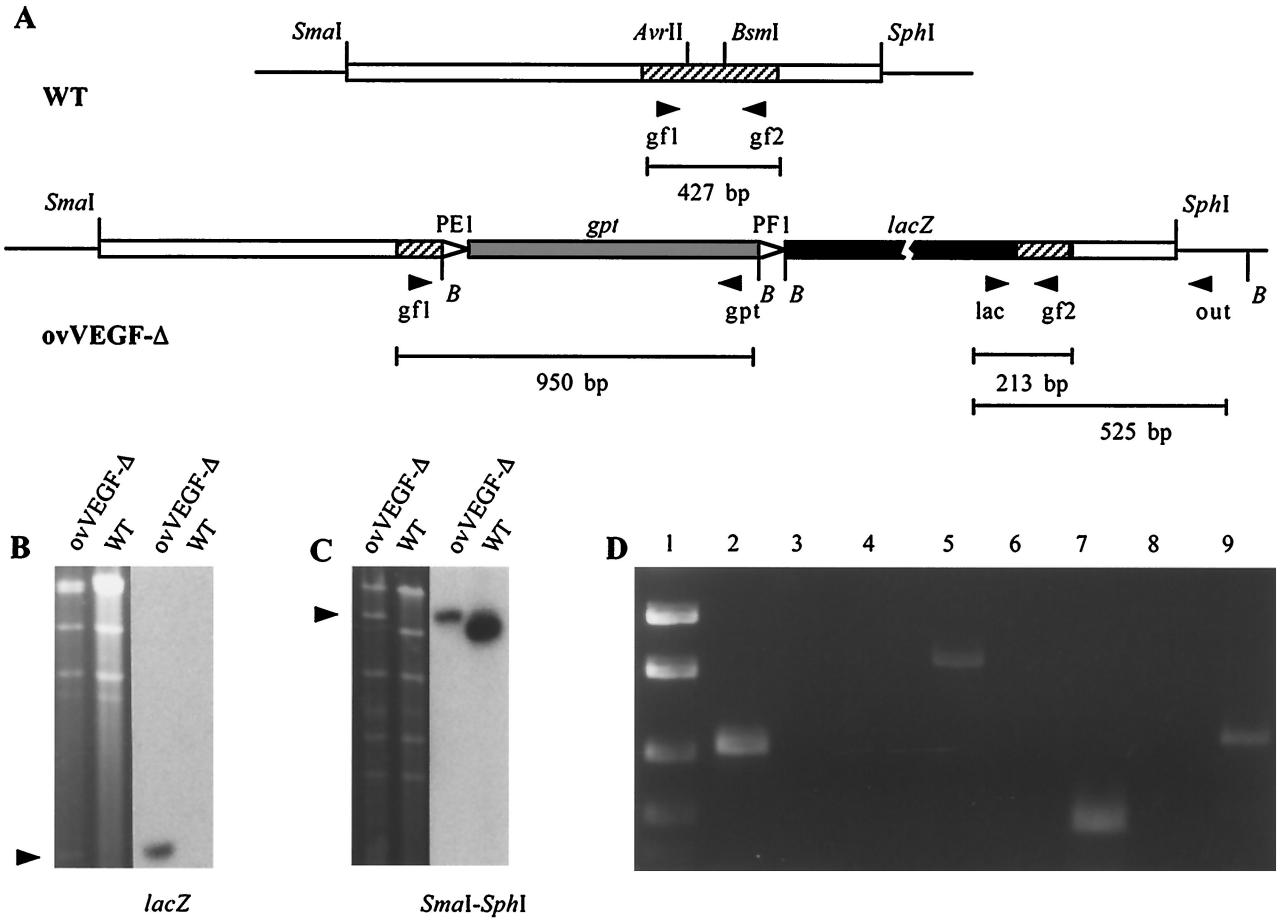


FIG. 1. Characterization of the orf virus recombinant, ovVEGF-Δ. (A) Schematic diagram showing the location of the VEGF gene (hatched bar) within a 1.45-kb *Sma*I-*Sph*I fragment of the orf virus genome (26). The region between the marked *Avr*II and *Bsm*I sites was deleted from the WT VEGF gene during the construction of ovVEGF-Δ. This region was replaced with the *gpt* and *lacZ* genes under the control of an orf virus early promoter (PE1) and a late promoter (PF1), respectively. The box representing *lacZ* is interrupted to indicate that it is not drawn to scale. The locations of four *Bam*HI sites are marked with *B*. The distances between these sites, from left to right, are 812, 111, and 5,414 bp. Arrowheads indicate the locations of PCR primers (see below). Sequences denoted as bars were included in the plasmid (pVEGF-Δ) used in the construction of ovVEGF-Δ. Horizontal lines extending from these boxes represent adjacent orf virus genome sequences not included in pVEGF-Δ. (B) *Bam*HI restriction endonuclease cleavage fragments derived from ovVEGF-Δ and WT genomic DNAs were separated on a 0.7% agarose gel (left panel). The 5.4-kb *Bam*HI fragment derived from ovVEGF-Δ is indicated by an arrowhead. The fragments were Southern blotted and hybridized with the *lacZ* probe (right panel). (C) *Hin*dIII restriction endonuclease cleavage fragments derived from ovVEGF-Δ and WT genomic DNAs were separated on a 0.7% agarose gel (left panel). The *Hin*dIII fragment unique to ovVEGF-Δ is indicated by an arrowhead. The fragments were Southern blotted and probed with a plasmid containing the 1.45-kb *Sma*I-*Sph*I fragment shown in panel A (right panel). (D) PCR products derived from WT and ovVEGF-Δ genomic DNAs were electrophoresed on a 1.3% agarose gel and visualized with ethidium bromide. The primer pairs used for PCR amplifications are indicated by arrowheads in panel A, and the bars below those arrowheads indicate the predicted sizes of the PCR products. Template DNA used in the reactions was WT DNA (even-numbered lanes) or ovVEGF-Δ DNA (odd-numbered lanes). Lane 1, low-DNA-mass ladder (Gibco BRL); bands of 1,200, 800, 400, and 200 bp are shown. Lanes 2 and 3, primers gf1 and gf2. Lanes 4 and 5, primers gf1 and gpt. Lanes 6 and 7, primers lac and gf2. Lanes 8 and 9, primers lac and out.

fold increase in the number of HMVEC (Fig. 2A). No such increase was promoted by CM from cells infected with ovVEGF-Δ or vaccinia virus or mock infected.

A bioassay based on a Ba/F3-derived cell line that responds to binding and cross-linking of VEGFR-2 is available. It has been shown that VEGF family members that bind VEGFR-2 can stimulate the growth of this cell line in a specific and dose-dependent fashion (37). Figure 2B shows that CM from WT-infected BT cells was active in the bioassay but that CM from BT cells infected with ovVEGF-Δ was not. CM from COS-7 cells transiently expressing mouse $VEGF_{164}$ was also able to stimulate thymidine incorporation by the Ba/F3-derived cells. CM from infected LT cells was assayed for the ability to induce vascular permeability in guinea pig skin. CM from WT-infected cells induced permeability, whereas CM from ovVEGF-Δ-, vaccinia virus-, and mock-infected cells did not (Fig. 2C). Mouse $VEGF_{164}$ (5 ng) served as a positive control in this assay. These data demonstrate that orf virus-infected cells express a product that stimulates VEGFR-2 and promotes both endothelial cell mitogenesis and vascular permeability but that this product is not produced by ovVEGF-Δ.

**Gross pathology of WT and ovVEGF-Δ lesions.** In order to assess the role of VEGF-$ORFV_{NZ2}$ in disease, we infected sheep by applying $10^6$ PFU of virus to scarified skin. Each of three animals was given four replicate inoculations with WT, ovVEGF-Δ, or PBS. The development of WT lesions followed the general pattern reported previously (24). This pattern was characterized by the progressive development of erythema, pustules, and a scab until the experiment was terminated 14 days p.i. Representative lesions observed on one animal are shown in Fig. 3A. Erythema was visible along the scratch lines 2 days p.i. This reaction was marked by 4 days, at which time

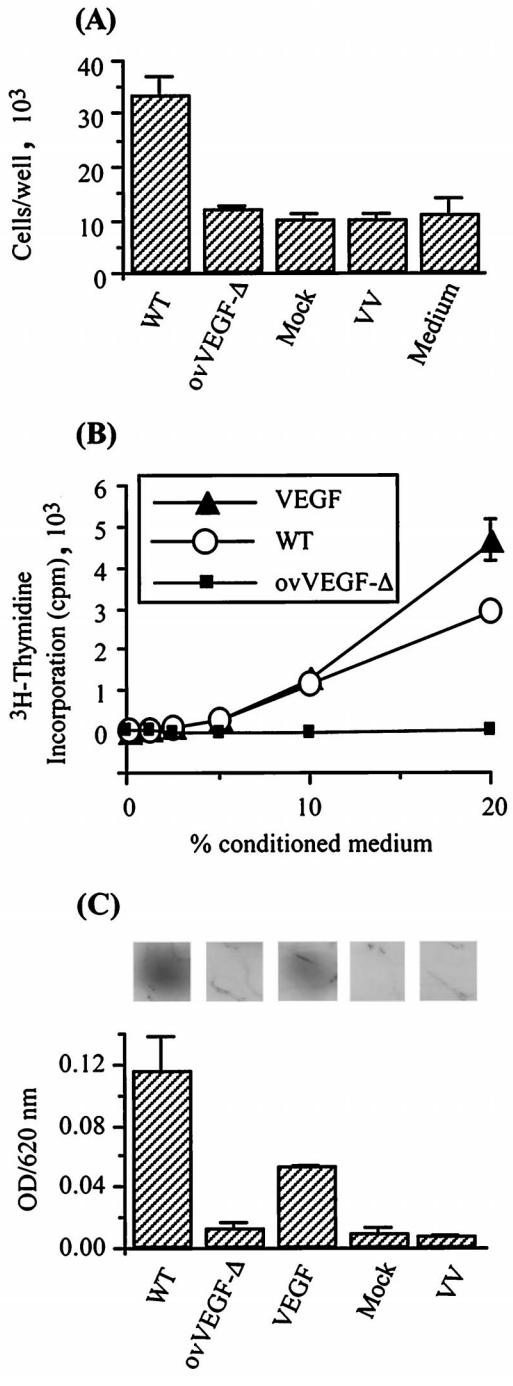


FIG. 2. VEGF activity is not produced by ovVEGF-Δ. CM was prepared from WT-, ovVEGF-Δ-, vaccinia virus (VV)-, and mock-infected cells. (A) Mitogenic activity of CM for endothelial cells. HMVEC were seeded at $10^4$ cells per well in medium supplemented (10%) with CM from the indicated source (LT cells were used), and cell numbers were determined after 72 h. Values are the mean ± standard deviation (SD) of triplicate experiments. (B) Activation of VEGFR-2 by CM. Ba/F3 cells expressing chimeric VEGFR-2 were resuspended in dilutions of CM from virus-infected BT cells (WT or ovVEGF-Δ) and from COS-7 cells transiently expressing mouse $VEGF_{164}$ (VEGF). Cells were incubated for 48 h, and DNA synthesis was quantified by measuring $^3$H-thymidine incorporation and β counting. Values are the mean ± SD of duplicate readings. (C) Induction of vascular permeability by CM (Miles assay). Guinea pigs were injected intracardially with Evans blue dye. CM (from LT cells) and 5 ng of purified mouse $VEGF_{164}$ (VEGF) were injected intradermally. After 20 min, the skin was excised and photographed (top), the dye was eluted in formamide, and the absorbance at 620 nm (OD/620 nm) was recorded (bottom). Values are the mean ± SD of duplicate injections.

pustules first became apparent (data not shown). By 6 days p.i., the intense erythematous margin seen after 4 days was still evident and the pustules had developed further. Pustule formation was at a maximum 10 days p.i., by which time the erythema was reduced. At the last time point, 14 days p.i., erythema was minimal, the pustules had contracted, and a scab was beginning to form.

Lesions induced by ovVEGF-Δ followed a course similar to that observed with infection by WT but were substantially less florid. Some reddening along the lines of ovVEGF-Δ infection was apparent 6 and 10 days p.i., but the marked erythematous reaction seen with WT was not evident. Pustule formation was minimal and was visible only 10 days p.i. A fine line of scab formed over mock-infected scratches, but there was no evidence of erythema or pustule formation. For all inoculations, there was good uniformity in the responses seen in the replicate lesions on individual animals and across all three animals.

**Histological analysis of WT and ovVEGF-Δ lesions.** The reduced pathology seen in superficial examinations of ovVEGF-Δ lesions compared with WT lesions was also apparent in histological examinations of these lesions (Fig. 3B). Histological differences were seen as early as 2 days p.i., when in the WT lesions there was an accumulation of fluid in the dermis that was not seen in the ovVEGF-Δ lesions or PBS controls. After 6 days, there was an intense influx of inflammatory cells in the dermis of WT lesions. Cellular ballooning and degeneration of the upper layers of the epidermis were also evident in WT lesions, and the epidermis had become markedly hyperplastic. In contrast, the influx of inflammatory cells into the dermis of ovVEGF-Δ lesions was less intense, and there was little evidence of the cytopathic effects observed in the epidermis of WT lesions.

Figure 3B shows sections of lesions sampled 10 days p.i. The regenerating epidermis of WT lesions had walled off the developing pustule that was heavily infiltrated with inflammatory cells and in some cases contained a fluid exudate. The new epidermis was extremely hyperplastic, and the levels of inflammatory cells in the dermis remained high. ovVEGF-Δ lesions at this stage had a relatively intense inflammatory cell infiltrate, the upper layers of the epidermis showed signs of degeneration, and the epidermis had become mildly hyperplastic. All ovVEGF-Δ lesions had developed a small pustule that had lifted away from the epidermis.

At 14 days p.i., the dermis of WT lesions remained heavily infiltrated with inflammatory cells, the epidermis was extremely hyperplastic, and the overlying pustule had become much larger and in some cases had detached. In contrast, ovVEGF-Δ lesions had a mild inflammatory cell infiltrate, any pustule that had been present had detached, and the epidermis remained mildly thickened and hyperplastic. In summary, both histological examinations and the observed gross pathology suggested that the inactivation of viral VEGF resulted in an infection that was substantially less intense and resolved more quickly.

**Epidermal hyperplasia in orf virus lesions.** Epidermal hyperplasia is a feature of the response to orf virus infection. At 14 days p.i., the epidermis of WT lesions was more than sevenfold thicker than that of mock-infected lesions and approximately twofold thicker than that of ovVEGF-Δ lesions (data not shown). A major component of the enlarged epidermis seen in WT lesions was the number of epidermal downgrowths, known as rete ridges. These were apparent 6 days p.i., when WT lesions had developed 9.3-fold more rete ridges than had ovVEGF-Δ lesions (Table 1). The rete ridges seen in WT lesions extended further into the dermis and were, on average, 1.7-fold longer than those few seen in ovVEGF-Δ lesions. This

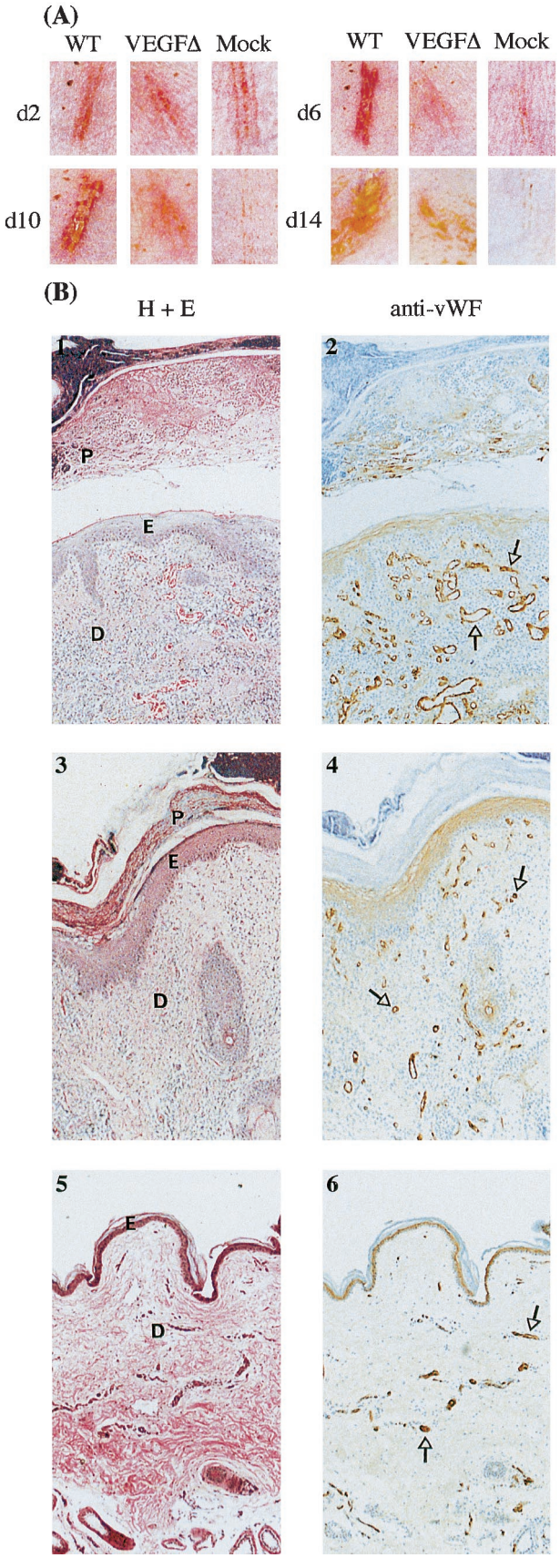


TABLE 1. Induction of rete ridges in skin infected by WT and ovVEGF-Δ (Rec)[a]

| Animal | Day p.i. | No. of rete ridges caused by: | | Length (μm) of rete ridges caused by: | |
|---|---|---|---|---|---|
| | | WT | Rec | WT | Rec |
| 101 | 6 | 35 | 2 | 106 ± 29 | 55 ± 7 |
| 102 | 6 | 40 | 3 | 250 ± 123 | 157 ± 35 |
| 103 | 6 | 27 | 6 | 196 ± 55 | 132 ± 28 |
| 101 | 14 | 38 | 9 | 424 ± 161 | 257 ± 63 |
| 102 | 14 | 29 | 1 | 389 ± 19 | 220 |
| 103 | 14 | 19 | 0 | 252 ± 65 | |

[a] The number of rete ridges is the total number seen on three sections of each 5-mm biopsy specimen. Ridge length is from basal layer to granular layer of the epidermis or to the highest point of intact epidermis. Values for ridge length are given as mean ± standard deviation. Mock-infected skin showed no rete ridges and had an average epidermal thickness of 28 μm (data not shown).

pattern was also apparent 14 days p.i., at which time the rete ridges had increased in length by two- to threefold over those seen at 6 days p.i. (Table 1). Rete ridges were not seen in mock-infected lesions.

**WT lesions are more vascularized than ovVEGF-Δ lesions.** Vascularization at the sites of infection was assessed using anti-human von Willebrand factor antibody. Representative sections from WT-, ovVEGF-Δ-, and mock-infected lesions sampled 10 days p.i. are shown in Fig. 3B. The extent of dermal vascularization associated with sites of infection was analyzed by determining the areal fraction of dermis reacting with anti-von Willebrand factor antibody. This quantitative analysis of vascularization showed a time-dependent increase in the dermal vascularization of WT lesions that greatly exceeded any such response in ovVEGF-Δ lesions (Fig. 4). At 2 days p.i., there appeared to be no difference in the vascularization of WT-, ovVEGF-Δ-, or mock-infected lesions. By 6 days p.i., however, the dermis of WT lesions was intensely vascularized and the lumen of blood vessels appeared to be enlarged. WT lesions were from 1.8-fold (sheep 102) to 3.8-fold (sheep 103) more vascularized than corresponding mock-infected lesions (Fig. 4). Markedly enhanced dermal vascularization and dilation of blood vessels were also apparent in WT lesions sampled 10 (Fig. 3) and 14 days p.i., with the area vascularized exceeding that seen in mock-infected lesions by an average of 5-fold and by as much as 9.8-fold in one case (sheep 101; day 14). It was clear that orf virus infection of sheep skin induced a substantial proliferation of the vasculature of the underlying dermis. This dramatic response was not seen in ovVEGF-Δ lesions. In all samples taken at days 6, 10, and 14 p.i., ovVEGF-Δ lesions were found to be less vascularized than WT lesions taken at the same time from the same animal (Fig. 4). At these

FIG. 3. Histopathological analysis of the role of VEGF-ORFV$_{NZ2}$ in infection of sheep. Scarified skin was inoculated with WT or ovVEGF-Δ (VEGFΔ) or mock infected. (A) Gross pathology. Representative lesions at 2, 6, 10, and 14 days (d) p.i., shown at approximately half life size. All lesions are from the same animal (101). (B) Histological comparison of WT-infected (panels 1 and 2), ovVEGF-Δ-infected (panels 3 and 4), and mock-infected (panels 5 and 6) lesions at 10 days p.i. (magnification, ×50). Panels 1, 3, and 5 show representative sections stained with hematoxylin and eosin (H + E), while panels 2, 4, and 6 show the adjacent sections from the same biopsy stained with peroxidase-conjugated anti-von Willebrand factor antibody (anti-vWF) and 3,3′-diaminobenzamine to reveal endothelial cells. The pustule (P), epidermis (E), and dermis (D) are indicated where appropriate, and arrows indicate representative blood vessels highlighted by the antibody staining.

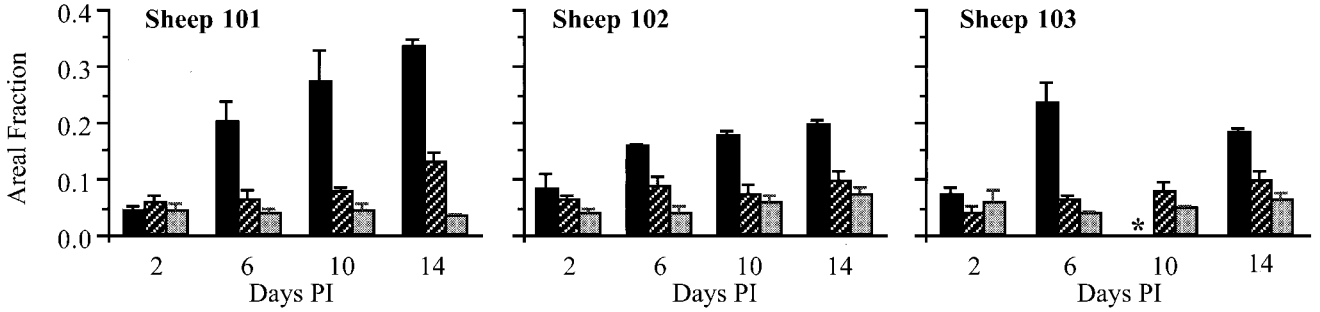


FIG. 4. Vascularization of orf virus lesions. Scarified skin was inoculated with WT (black), ovVEGF-Δ (hatched bars), and PBS (grey bars). Five-millimeter punch biopsies were taken from separate lesions of each animal at days 2, 6, 10, and 14 p.i. The dermal areal fraction reacting with anti-von Willebrand factor antibody was calculated from the analysis of three equidistant sections as outlined in Materials and Methods. Values are the mean ± standard deviation. The asterisk indicates that no data were obtained from this biopsy, but regression methods were used to derive an estimate of 0.24; this value was used in subsequent analyses.

times p.i., the extent of dermal vascularization of the WT lesions exceeded that seen in the corresponding ovVEGF-Δ lesions by 1.9- to 6.2-fold. Analysis of these data using paired *t* tests for each day confirmed that the vascularization seen in WT lesions was significantly greater than that seen in ovVEGF-Δ lesions at 6, 10, and 14 days p.i. (*P* values of 0.048, 0.021, and 0.039, respectively) but was not significantly different at 2 days p.i. (*P* value of 0.485). Figure 4 shows that in all samples taken 6, 10, and 14 days p.i., the extent of dermal vascularization recorded for ovVEGF-Δ lesions exceeded that recorded for mock-infected lesions. This stimulation of vascularization was markedly lower than that seen for WT lesions and, on average, the values for ovVEGF-Δ infection exceeded those for mock infection by 1.7-fold. Only vascularization at 6 days p.i. was significantly different (*P* value of 0.039). These results demonstrate that the viral VEGF is expressed during natural infection and plays a key role in the development of the vascularized nature of orf virus lesions.

**Effect of inactivation of VEGF-ORFV$_{NZ2}$ on viral yield in vivo.** In order to provide an estimate of the production of infectious virus during the course of infection in sheep skin, 3-mm punch biopsies were taken and, after processing, the titers of PFU were determined (Fig. 5). At 2 days p.i., virus was detected in only two of the six samples, but by 6 days p.i., all viral lesions contained significant amounts of virus, with similar titers of virus being detected in WT and ovVEGF-Δ lesions. This result can be seen in the average ratio of WT to ovVEGF-Δ titers, which at day 6 was 0.9.

The strong growth of ovVEGF-Δ was somewhat unexpected in light of the reduced pathology of the lesions. The results indicate that in the absence of a functional VEGF-like gene and the consequent absence of extensive dermal vascularization, ovVEGF-Δ can establish an infection that, in terms of viral yield during the early stages, is similar to that established by WT. Viral titers in WT lesions sampled 10 or 14 days p.i. were generally higher than the day-6 titers, with an average 20.2-fold increase between day-6 titers and maximum titers. In contrast to the uniform increase in the titers in WT lesions, the titers in ovVEGF-Δ lesions on two sheep were reduced in samples taken later than 6 days p.i. Furthermore, in no case did the titers in samples taken from ovVEGF-Δ lesions 10 and 14 days p.i. exceed the titers in samples taken from WT lesions on the same sheep at the same time. This result suggested that at later stages of the infection, the growth of ovVEGF-Δ was impaired relative to that of WT. However, analysis by paired *t* tests revealed that only the difference seen 10 days p.i. was statistically significant (*P* value of 0.039).

X-Gal staining of plaques derived from the biopsies of ovVEGF-Δ lesions revealed that the *lacZ* gene had been retained in the progeny virus. PCR analysis of WT and ovVEGF-Δ biopsy specimens using the primer pairs gf1-gf2 and *lacZ*-gf2 (Fig. 1), followed by sequencing of products, confirmed the absence of the VEGF-like gene in virus recovered from ovVEGF-Δ lesions.

## DISCUSSION

Descriptions of orf virus lesions frequently refer to prominent vascular changes, and as early as 1890, Walley referred to lesions that "readily bleed" and observed "distension of the

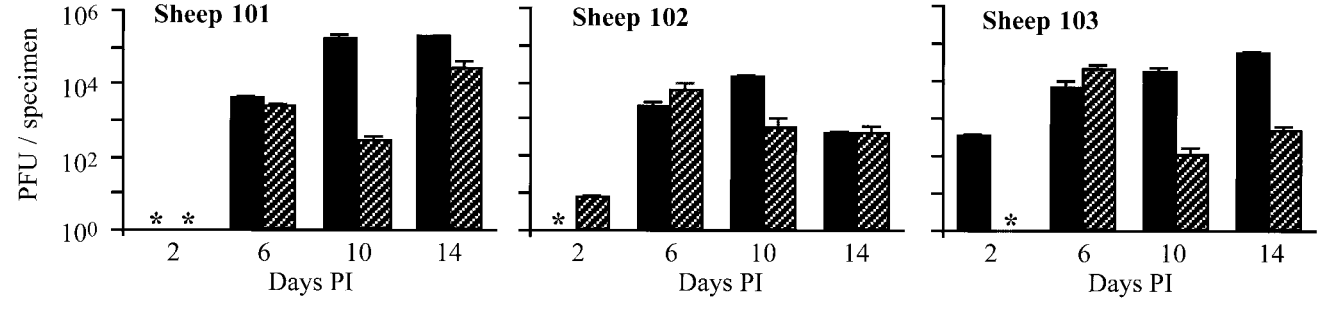


FIG. 5. Effect of inactivation of VEGF-ORFV$_{NZ2}$ on virus yield in infected sheep. Scarified skin was inoculated with WT (black bars) and ovVEGF-Δ (hatched bars). Three-millimeter punch biopsies were taken from separate lesions of each animal at days 2, 6, 10, and 14 p.i. Samples were processed and viral titers were determined as described in Materials and Methods. Values are the mean ± standard deviation of duplicate titrations. Asterisks indicate that the viral titer was less than 5 PFU per sample.

blood vessels" (41). More recently, Groves described "massive capillary proliferation and dilation [that] gave the impression of an angiomatous lesion" (18). Construction of a recombinant orf virus in which the viral VEGF was inactivated allowed us to examine for the first time the role played by the viral VEGF in the vascular response seen in orf virus lesions.

We demonstrate here that VEGF-like activities expressed by WT-infected cells were not seen in cells infected with the recombinant virus, in which the VEGF-like gene was disrupted. Disruption of the viral VEGF gene and the loss of VEGF activity had no detectable effect on the growth of orf virus in cultured cells; however, infection of its natural host was significantly affected. Analysis of vascularization associated with the viral lesions allowed us to confirm previous reports that the dermis underlying an orf virus lesion is intensely vascularized (18). As early as 6 days p.i., the density of endothelial cells was, on average, fivefold greater than that seen in the dermis of a mock-infected lesion. Furthermore, at this time and up to at least 14 days p.i., there was significantly greater vascularization of WT lesions than of lesions induced by ovVEGF-Δ. These observations demonstrate that the viral VEGF is able to promote angiogenesis during infection of skin.

Although our measure of the vascular response was based on the density of endothelial cells rather than on vascular profiles, we did observe a progressive development of recognizable microvessels with clearly visible lumina (Fig. 3). Confirmation that the vast majority of the vascular response is directed by the viral VEGF rather than by host factors induced by orf virus infection is provided by the virus yield data, which show that at 6 days p.i., the virus yields are similar for both WT and ovVEGF-Δ. If dermal vascularization were a host response to viral infection, it would be expected that the response would be proportional to the extent of viral growth. This is clearly not so. Orf virus replication is known to be confined to the epidermis (23, 24), but our data suggest that the viral VEGF affects endothelial cells of the dermis. This notion is consistent with the results of studies of transgenic mice, in which overexpression of VEGF in keratinocytes stimulated an increase in the density of blood vessels in the dermis (10). Enhanced expression of VEGF has also been reported for a range of malignant and benign tumors of the skin and has been shown for advanced melanoma lesions to directly correlate with a 2.5-fold increase in the vascular density of the associated dermis (11). Studies with purified VEGF-ORFV$_{NZ2}$ have shown that it recognizes VEGFR-2 but not VEGFR-1 or VEGFR-3 (31, 43). Our demonstration that in situ expression of this factor promotes angiogenesis is consistent with the view that VEGFR-2 is predominantly responsible for signaling vascular endothelial cell mitogenesis.

Our data show a correlation between the presence of an intact viral VEGF gene and the induction of not only dermal vascularization but also epidermal hyperplasia. Cutaneous angiogenesis in conjunction with epidermal hyperplasia has also been reported for cutaneous infantile hemangiomas and UV-irradiated skin and was connected in both studies to altered levels of angiogenic factors, including VEGF (3, 4). The pathway by which the viral VEGF might induce epidermal proliferation is unclear, but the induction of growth factors, such as fibroblast growth factor 2 (FGF-2), keratinocyte growth factor (KGF), or heparin-binding epidermal growth factor (HB-EGF), is possible. For example, VEGF has been shown to induce HB-EGF in vascular endothelial cells, and HB-EGF is a known mitogen of keratinocytes (2).

In addition to a general thickening of the epidermis, WT lesions showed extensive rete ridge formation that was not apparent in ovVEGF-Δ lesions. These extensions of the epidermis into the dermis are also seen in other pathologies. For example, psoriatic skin shows both enhanced angiogenesis and an increase in rete ridge length (9). A link between rete ridge formation and KGF was suggested by a study of wound healing (38). A role for the orf virus-encoded VEGF in promoting the expression of KGF could be postulated to occur via increased vascular permeability, leading to alterations in the dermal extracellular matrix, including the release of sequestered FGF-2. Such FGF-2 could then signal dermal fibroblasts to produce KGF and might thereby induce epidermal proliferation, with the formation of rete ridges.

The considerable epidermal proliferation seen in ovVEGF-Δ lesions indicates that factors other than VEGF-ORFV$_{NZ2}$ also play a role in stimulating this cellular response to orf virus infection. Lesions of other poxviruses typically demonstrate localized cellular proliferation but do not show the vascularization seen in orf virus lesions. A probable explanation for this effect has been provided by the demonstration that several poxviruses each encode a growth factor related to epidermal growth factor (EGF) (5, 8, 40). We have not been able to detect any evidence of an EGF homolog encoded by orf virus. Nor is there any evidence of VEGF-like activity encoded by any virus other than parapoxviruses. However, virus-encoded EGF and VEGF are both examples of a growing family of factors which are expressed by poxviruses and other large DNA viruses, which are often nonessential for viral replication, but which play important roles in modulating the host environment during infection (25, 28, 36).

The epidermal and vascular responses seen in lesions of orf virus are reminiscent of a sustained wound healing response. Orf virus applied to wounded skin establishes replication in the regenerating epidermal layer (23, 24), and extravagantly proliferative and persistent orf virus lesions have been reported for immunocompromised individuals (21, 35, 39). The expression of a viral VEGF might assist in maintaining this regenerative response and thereby might support extended viral growth. Our data are suggestive of extended replication of WT relative to orf virus with a deletion of VEGF, but more detailed examinations will be required to clarify this possibility. Atypically severe orf virus lesions have been reported for thermally injured skin (20), and erythema multiforme reactions are a relatively common complication of orf virus infection. Intriguingly, both of these pathologies, in the absence of orf virus, have been linked to elevated levels of VEGF (6, 17).

Another possible role for the viral VEGF, again with a link to wound healing, is the extensive scab formation seen on healing orf virus lesions. The scab shed from orf virus lesions contains substantial amounts of infectious virus. The envelopment of the virus in the scab provides it with protection from environmental inactivation. In this way, the virus remains available to infect naive animals as much as 1 year after being shed (19). Vascular hyperpermeability, with associated leakage of plasma proteins, is a feature of wound healing and has been linked to the overexpression of VEGF (7). The viral VEGF is able to induce vascular permeability and would seem to contribute to scab formation, since lesions induced by orf virus with a deletion of VEGF have essentially no scab. Our data conclusively demonstrate an in vivo role for the virus-encoded VEGF and provide a natural disease model to study the activities of a new member of the VEGF family that activates VEGFR-2 but not VEGFR-1 or VEGFR-3.

## ACKNOWLEDGMENTS

This work was supported in part by the Health Research Council of New Zealand.

We thank D. Lyttle for supplying genetic elements used in the

construction of pVEGF-Δ; C. Macintosh for assistance with the sheep studies; R. Napper, K. Turner, and H.-S. Yoon for assistance with histological analyses; N. Ferrara for preliminary analysis of orf virus-encoded VEGF activity; L. Wise for useful discussions; and E. Whelan, C. Caesar, and A. Vitali for skilled technical assistance.

## REFERENCES


1. **Achen, M. G., and S. A. Stacker.** 1998. The vascular endothelial growth factor family; proteins which guide the development of the vasculature. Int. J. Exp. Pathol. **79:**255–265.
2. **Arkonac, B. M., L. C. Foster, N. E. Sibinga, C. Patterson, K. Lai, J. C. Tsai, M. E. Lee, M. A. Perrella, and E. Haber.** 1998. Vascular endothelial growth factor induces heparin-binding epidermal growth factor-like growth factor in vascular endothelial cells. J. Biol. Chem. **273:**4400–4405.
3. **Bielenberg, D. R., C. D. Bucana, R. Sanchez, C. K. Donawho, M. L. Kripke, and I. J. Fidler.** 1998. Molecular regulation of UVB-induced cutaneous angiogenesis. J. Investig. Dermatol. **111:**864–872.
4. **Bielenberg, D. R., C. D. Bucana, R. Sanchez, J. B. Mulliken, J. Folkman, and I. J. Fidler.** 1999. Progressive growth of infantile cutaneous hemangiomas is directly correlated with hyperplasia and angiogenesis of adjacent epidermis and inversely correlated with expression of the endogenous angiogenesis inhibitor, IFN-beta. Int. J. Oncol. **14:**401–408.
5. **Blomquist, M. C., L. T. Hunt, and W. C. Barker.** 1984. Vaccinia virus 19-kilodalton protein: relationship to several mammalian proteins, including two growth factors. Proc. Natl. Acad. Sci. USA **81:**7363–7367.
6. **Brown, L. F., T. J. Harrist, K. T. Yeo, M. Stahle-Backdahl, R. W. Jackman, B. Berse, K. Tognazzi, H. F. Dvorak, and M. Detmar.** 1995. Increased expression of vascular permeability factor (vascular endothelial growth factor) in bullous pemphigoid, dermatitis herpetiformis, and erythema multiforme. J. Investig. Dermatol. **104:**744–749.
7. **Brown, L. F., K. T. Yeo, B. Berse, T. K. Yeo, D. R. Senger, H. F. Dvorak, and L. van de Water.** 1992. Expression of vascular permeability factor (vascular endothelial growth factor) by epidermal keratinocytes during wound healing. J. Exp. Med. **176:**1375–1379.
8. **Chang, W., C. Upton, S. L. Hu, A. F. Purchio, and G. McFadden.** 1987. The genome of Shope fibroma virus, a tumorigenic poxvirus, contains a growth factor gene with sequence similarity to those encoding epidermal growth factor and transforming growth factor alpha. Mol. Cell. Biol. **7:**535–540.
9. **Dam, T. N., S. Kang, B. J. Nickoloff, and J. J. Voorhees.** 1999. 1α,25-Dihydroxycholecalciferol and cyclosporine suppress induction and promote resolution of psoriasis in human skin grafts transplanted on to SCID mice. J. Investig. Dermatol. **113:**1082–1089.
10. **Detmar, M., L. F. Brown, M. P. Schon, B. M. Elicker, P. Velasco, L. Richard, D. Fukumura, W. Monsky, K. P. Claffey, and R. K. Jain.** 1998. Increased microvascular density and enhanced leukocyte rolling and adhesion in the skin of VEGF transgenic mice. J. Investig. Dermatol. **111:**1–6.
11. **Erhard, H., F. J. Rietveld, M. C. van Altena, E. B. Brocker, D. J. Ruiter, and R. M. de Waal.** 1997. Transition of horizontal to vertical growth phase melanoma is accompanied by induction of vascular endothelial growth factor expression and angiogenesis. Melanoma Res. **7**(Suppl. 2)**:**S19–S26.
12. **Esposito, J., R. Condit, and J. Obijeski.** 1981. The preparation of orthopoxvirus DNA. J. Virol. Methods **2:**175–179.
13. **Ferrara, N., and T. Davis-Smyth.** 1997. The biology of vascular endothelial growth factor. Endocrine Rev. **16:**4–25.
14. **Fleming, S. B., J. Blok, K. M. Fraser, A. A. Mercer, and A. J. Robinson.** 1993. Conservation of gene structure and arrangement between vaccinia virus and orf virus. Virology **195:**175–184.
15. **Fleming, S. B., K. M. Fraser, A. A. Mercer, and A. J. Robinson.** 1991. Vaccinia virus-like early transcriptional control sequences flank an early gene in orf virus. Gene **97:**207–212.
16. **Fleming, S. B., C. A. McCaughan, A. E. Andrews, A. D. Nash, and A. A. Mercer.** 1997. A homolog of interleukin-10 is encoded by the poxvirus orf virus. J. Virol. **71:**4857–4861.
17. **Grad, S., W. Ertel, M. Keel, M. Infanger, D. J. Vonderschmitt, and F. E. Maly.** 1998. Strongly enhanced serum levels of vascular endothelial growth factor (VEGF) after polytrauma and burn. Clin. Chem. Lab. Med. **36:**379–383.
18. **Groves, R. W.** 1991. Human orf and milkers' nodule: a clinicopathological study. J. Am. Acad. Dermatol. **25:**706–711.
19. **Haig, D. M., and A. A. Mercer.** 1998. Orf. Vet. Res. **29:**311–326.
20. **Hooser, S. B., G. Scherba, D. E. Morin, and H. E. Whiteley.** 1989. Atypical contagious ecthyma in a sheep after extensive cutaneous thermal injury. J. Am. Vet. Med. Assoc. **195:**1255–1256.
21. **Hunskaar, S.** 1986. Giant orf in a patient with lymphocytic leukaemia. Br. J. Dermatol. **114:**631–634.
22. **Hussain, K. A., and D. Buger.** 1989. *In vivo* and *in vitro* characteristics of contagious ecthyma virus isolates: host response mechanism. Vet. Microbiol. **19:**23–26.
23. **Jenkinson, D. M., P. E. McEwan, V. A. Moss, H. Y. Elder, and H. W. Reid.** 1990. Location and spread of orf virus antigen in infected ovine skin. Vet. Dermatol. **1:**189–195.
24. **Jenkinson, D. M., P. E. McEwan, S. K. Onwuka, V. A. Moss, H. Y. Elder, G. Hutchinson, and H. W. Reid.** 1990. The pathological changes and polymorphonuclear and mast cell responses in the skin of specific pathogen free lambs following primary and secondary challenge with orf virus. Vet. Dermatol. **1:**139–150.
25. **Kalvakolanu, D. V.** 1999. Virus interception of cytokine-regulated pathways. Trends Microbiol. **7:**166–171.
26. **Lyttle, D. J., K. M. Fraser, S. B. Fleming, A. A. Mercer, and A. J. Robinson.** 1994. Homologs of vascular endothelial growth factor are encoded by the poxvirus orf virus. J. Virol. **68:**84–92.
27. **Mackett, M., G. L. Smith, and B. Moss.** 1984. A general method for the production and selection of infectious vaccinia virus recombinants expressing foreign genes. J. Virol. **49:**857–864.
28. **McFadden, G., K. Graham, K. Ellison, M. Barry, J. Macen, M. Schreiber, K. Mossman, P. Nash, A. Lalani, and H. Everett.** 1995. Interruption of cytokine networks by poxviruses: lessons from myxoma virus. J. Leukoc. Biol. **57:**731–738.
29. **Mercer, A. A., K. F. Fraser, G. Barns, and A. J. Robinson.** 1987. The structure and cloning of orf virus DNA. Virology **157:**1–12.
30. **Mercer, A. A., D. J. Lyttle, E. M. Whelan, S. B. Fleming, and J. T. Sullivan.** 1995. The establishment of a gene map of orf virus reveals a pattern of genomic organisation that is highly conserved among divergent poxviruses. Virology **212:**698–704.
31. **Meyer, M., M. Clauss, A. Lepple-Wienhues, J. Waltenberger, H. G. Augustin, M. Ziche, C. Lanz, M. Büttner, H.-J. Rziha, and C. Dehio.** 1999. A novel vascular endothelial growth factor encoded by orf virus, VEGF-E, mediates angiogenesis via signalling through VEGFR-2 (KDR) but not VEGFR-1 (Flt-1) receptor tyrosine kinase. EMBO J. **18:**363–374.
32. **Moss, B.** 1996. Poxviridae and their replication, p. 2637–2671. *In* B. N. Fields, D. M. Knipe, and P. Howley (ed.), Fields virology, 3rd ed., vol. 2. Lippincott-Raven Publishers, Philadelphia, Pa.
33. **Robinson, A. J., G. Ellis, and T. Balassu.** 1982. The genome of orf virus: restriction endonuclease analysis of viral DNA isolated from lesions of orf virus in sheep. Arch. Virol. **71:**43–55.
34. **Robinson, A. J., and A. A. Mercer.** 1988. Orf virus and vaccinia virus do not cross protect in sheep. Arch. Virol. **101:**255–259.
35. **Savage, J., and M. M. Black.** 1972. "Giant orf" of finger in a patient with a lymphoma. Proc. R. Soc. Med. **64:**766–768.
36. **Smith, G. L., J. A. Symons, A. Khanna, A. Vanderplasschen, and A. Alcami.** 1997. Vaccinia virus immune evasion. Immunol. Rev. **159:**137–154.
37. **Stacker, S. A., A. Vitali, C. Caesar, T. Domagala, L. C. Groenen, E. Nice, M. G. Achen, and A. F. Wilks.** 1999. A mutant form of vascular endothelial growth factor (VEGF) that lacks VEGF receptor-2 activation retains the ability to induce vascular permeability. J. Biol. Chem. **274:**34884–34892.
38. **Staiano-Coico, L., J. G. Krueger, J. S. Rubin, S. D'Limi, V. P. Vallat, L. Valentino, T. D. Fahey, A. Hawes, G. Kingston, M. R. Madden, M. Mathwich, A. B. Gottlieb, and S. A. Aaronson.** 1993. Human keratinocyte growth factor effects in a porcine model of epidermal wound healing. J. Exp. Med. **178:**865–878.
39. **Tan, S. T., G. B. Blake, and S. Chambers.** 1991. Recurrent orf in an immunocompromised host. Br. J. Plastic Surg. **44:**465–467.
40. **Upton, C., J. L. Macen, and G. McFadden.** 1987. Mapping and sequencing of a gene from myxoma virus that is related to those encoding epidermal growth factor and transforming growth factor alpha. J. Virol. **61:**1271–1275.
41. **Walley, T.** 1890. Contagious dermatitis: "orf" in sheep. J. Comp. Pathol. Ther. **3:**357–360.
42. **Weidner, N., J. P. Semple, W. R. Welch, and J. Folkman.** 1991. Tumor angiogenesis and metastasis—correlation in invasive breast carcinoma. N. Engl. J. Med. **324:**1–8.
43. **Wise, L., T. Veikkola, A. Mercer, L. Savory, S. Fleming, C. Caesar, A. Vitali, T. Makinen, K. Alitalo, and S. Stacker.** 1999. Vascular endothelial growth factor (VEGF)-like protein from orf virus NZ2 binds to VEGFR-2 and neuropilin-1. Proc. Natl. Acad. Sci. USA **96:**3071–3076.
44. **Wittek, R., C. C. Kuenzle, and R. Wyler.** 1979. High G+C content in parapoxvirus DNA. J. Gen. Virol. **43:**231–234.